CONTROL OF CYTOPLASMIC CALCIUM WITH PHOTOLABILE TETRACARBOXYLATE 2-NITROBENZHYDROL CHELATORS

ROGER Y. TSIEN AND ROBERT S. ZUCKER
Department of Physiology-Anatomy, University of California, Berkeley, California 94720

ABSTRACT This paper introduces nitr-2, a new Ca^{2+} chelator designed to release Ca^{2+} upon illumination with near UV (300–400 nm) light. Before illumination nitr-2 has Ca^{2+} dissociation constants of 160 and 630 nM in 0.1 and 0.3 M ionic strength respectively; after photoconversion to a nitrosobenzophenone the values shift to 7 and 18 μM, high enough to liberate substantial amounts of Ca^{2+} under intracellular conditions. The speed of release is limited by a dark reaction with rate constant 5 s^{-1}. *Aplysia* central neurons injected with nitr-2 and exposed to UV light exhibit two separate Ca^{2+}-dependent membrane currents: one carried by potassium ions and one a nonspecific cation current. A quantitative estimate of the spatial distribution of intracellular [Ca^{2+}] changes in large cells filled with a high concentration of nitr-2 and exposed to an intense UV flash is offered.

INTRODUCTION

Many cellular processes are regulated or modulated by changes in intracellular Ca^{2+} activity. In order to study them, we must be able to manipulate cytoplasmic [Ca^{2+}]. A number of methods are presently available for this purpose: (*a*) Ca^{2+} can be released from internal organelles, such as mitochondria, by administering metabolic poisons (Bygrave, 1978). (*b*) Ca^{2+} transport across external or internal membranes can be increased with Ca^{2+}-carrying ionophores such as ionomycin and A23187 (Reed and Lardy, 1972; Liu and Hermann, 1978). (*c*) In some cells, Ca^{2+} influx through voltage-dependent channels can be evoked by membrane depolarization (Hagiwara and Byerly, 1981). (*d*) Ca^{2+} or Ca^{2+}-buffered solutions can be injected from a micropipette by pressure or iontophoresis (Curtis, 1964; Corson and Fein, 1983).

These methods are all subject to serious limitations: (*a* and *b*) Metabolic poisons and ionophores often have nonspecific effects, act slowly and irreversibly, and cannot be used to provide easily graded effects. (*c*) Not all cells have excitable Ca^{2+} channels, and depolarization of the cells may have other effects. The rise in intracellular Ca^{2+} due to influx through Ca^{2+} channels is initially restricted to the submembrane cytoplasmic region, and inactivation of Ca^{2+} channels limits the duration of Ca^{2+} influx. (*d*) Finally, Ca^{2+} microinjection pipettes are notoriously subject to clogging, and are limited by low transport numbers and hydrodynamic conductances for Ca^{2+} solutions. Injection at one point results in large internal spatial Ca^{2+} gradients, consequently the response depends critically on the location of the pipette tip with respect to the sites of Ca^{2+} action. Nevertheless, this is usually the best and most commonly employed technique for large cells. None of the available methods allow quantitative manipulation of intracellular Ca^{2+}, with reproducible known changes in [Ca^{2+}].

In this paper, we report a new method for changing intracellular [Ca^{2+}]. We introduce a Ca^{2+} chelator ("nitr-2") which is photo-isomerizable to a form with a much lower affinity for Ca^{2+}. A cell may be injected with Ca^{2+} bound to the chelator. When the chelator is exposed to light of the correct wavelength, Ca^{2+} is released from the chelator throughout the cytoplasm, and Ca^{2+}-dependent processes may be monitored during and after light exposure. The method is broadly analogous to the photochemical release of ATP or cyclic nucleotides reviewed recently (Lester and Nerbonne, 1982).

Fig. 1 shows the structure of nitr-2 and outlines the probable mechanism by which it releases Ca^{2+} upon illumination. Nitr-2 consists of BAPTA, a known Ca^{2+}-selective chelating structure (Tsien, 1980), linked to a nitropiperonyl group. Molecules with nitro groups *ortho* to

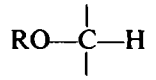

groups are well known to be photolyzable (reviewed by Pillai, 1980). The photochemical reaction mechanism has the eventual effect of inserting an oxygen atom from the nitro group into the adjacent C—H bond. This mechanism applied to nitr-2 gives the middle structure in Fig. 1, a hemiketal because of its

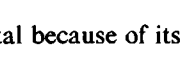

Such hemiketals in turn spontaneously release one mole of an alcohol to form a ketone, in this case the nitrosobenzophenone at the right of Fig. 1. For a closely analogous transformation, see Patchornik et al. (1970). Because of

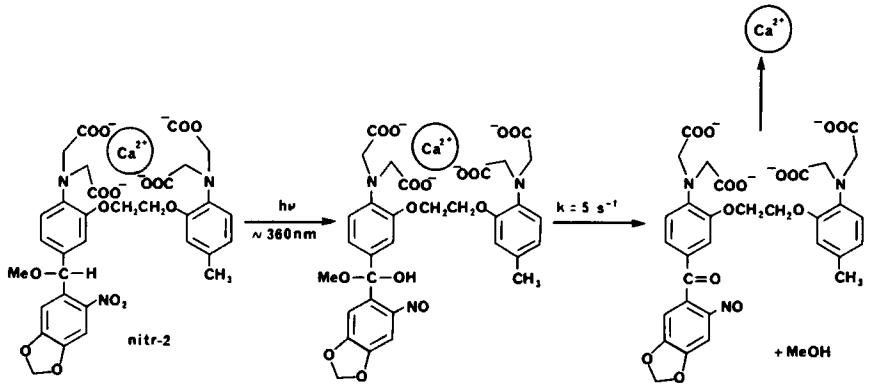

FIGURE 1 Structure of nitr-2 and presumed mechanism for its release of Ca^{2+} upon illumination. Nitr-2 is shown as its Ca^{2+} complex at the left; the BAPTA portion (Tsien, 1980) of the molecule corresponds to everything above the MeO—C—H, while the nitropiperonyl is everything below. Photolysis is presumed to go through very short-lived intermediates (not shown) to the hemiketal in the middle. Though an oxygen has been transferred from the nitro group into the C—H bond, no major change in spectra or Ca^{2+} affinity is expected. The hemiketal spontaneously eliminates MeOH in a dark reaction, producing the nitrosobenzophenone at far right, whose UV absorbance and Ca^{2+} dissociation constant greatly exceed those of nitr-2.

the electron withdrawing power of the newly formed carbonyl group, the nitrosobenzophenone has a much weaker affinity for Ca^{2+} than nitr-2 had.

METHODS

Synthesis

The tetraethyl esters of nitr-1 and nitr-2 were prepared by reacting 1-(2-bis(ethoxycarbonylmethyl)aminophenoxy)-2-(2-bis(ethoxycarbonylmethyl)amino-5-methylphenoxy)ethane, structure VIa of the Supplementary Material in Grynkiewicz et al. (1985), with the dimethyl acetals of 2-nitrobenzaldehyde or 6-nitropiperonal respectively. The reaction is driven forward by the selective Lewis acid trimethylsilyl trifluoromethanesulfonate (TMS OTf) and the hindered base 2,6-di-tert-butylpyridine. For example, 602 mg (1 mmol) of the amine substrate and 0.4 ml 2,6-di-tert-butylpyridine were dissolved in 10 ml dry dichloromethane under nitrogen and cooled to 0°C. To this mixture was added 0.3 ml TMS OTf in one portion. After 10 min, 0.4 g of 6-nitropiperonal dimethyl acetal dissolved in 5 ml dichloromethane was added dropwise from a syringe over 40 min. From this point onwards, the mixture was protected from short-wavelength light by wrapping the glassware in aluminum foil and working under an orange safelight. The reaction was stirred at 0°C for 3 h more, then diluted with dichloromethane and washed with aqueous $NaHCO_3$. The organic layer was dried over sodium sulfate, filtered, evaporated, and chromatographed on silica gel, eluting with a toluene-ethyl acetate mixture (4:1, vol/vol). The yield was 0.598 g, 74% of theoretical, in the form of a resin, pure by thin-layer chromatography and NMR except for a trace of toluene. The NMR spectrum in deuteriochloroform at 90 MHz showed multiplets at δ = 7.3–7.1 and 6.9–6.6, singlets at 6.0 and 5.88, a multiplet at 4.3–3.9, singlets at 3.29 and 2.20, and a 7 Hz triplet at 1.12. This material was eventually crystallized from di-isopropyl ether and had a melting point of 89–90°C.

The 6-nitropiperonal dimethyl acetal needed above was prepared from 6-nitropiperonal, excess methoxytrimethylsilane, and TMS OTf according to the general procedure of Noyori et al. (1981).

Nitr-2 tetraethyl ester was hydrolyzed to the free chelator tetra-anion by NaOH or KOH. For example, 55.3 mg (0.068 mmol) ester was dissolved in 1 ml warm ethanol and treated with 340 μl 1.0 M KOH all at once. After standing overnight at room temperature in the dark, the solvent was evaporated under vacuo and the residue rediluted with water to give a nitr-2 concentration of several hundred millimoles per liter. Solutions intended for microinjection into cells were supplemented with $CaCl_2$, usually to 75% of the nitr-2 concentration, and excess basicity neutralized with a chip of solid CO_2.

Calcium Affinities

Ca^{2+}-binding constants for nitr-2 before and after photolysis were determined by monitoring UV spectra during titration of N-(2-hydroxyethyl)ethylenediamine-N,N',N'-triacetic acid (HEEDTA) buffers to varying free Ca^{2+} levels. Either the ratio of [CaHEEDTA] to unbound [HEEDTA] was adjusted at a constant pH of 7.30, or the pH was varied while [CaHEEDTA] = [HEEDTA]. The equivalence of these approaches for pH >7 stems from the pH-insensitivity of BAPTA-like ligands. In 0.1 M KCl at room temperature, the logarithm of the effective affinity of HEEDTA for Ca^{2+} was calculated from the data of Martell and Smith (1974) to equal pH −1.70. In 0.1 M KCl + 0.18 M KOH + sufficient HEPES free acid to bring the pH to 7.30, the effective affinity of HEEDTA for Ca^{2+} at 18°C was taken as $1.84 \times 10^5\ M^{-1}$ (DiPolo et al., 1983).

Quantum Efficiencies

The quantum efficiencies of nitr-2 photolyses were mostly determined by irradiating a buffered solution of the substrate with a known intensity of long-wave ultraviolet light from a UVGL-58 hand mercury lamp (Ultraviolet Products, San Gabriel, CA). The output from this lamp peaked at the 365 nm Hg line but included a substantial contribution from a bell-shaped spectral distribution whose wavelengths at half-maximal intensity were 338 and 375 nm. Its total UV intensity was measured by actinometry with 6 mM potassium ferrioxalate (Hatchard and Parker, 1956) each experimental day. These intensities were around 10^{-8} einsteins · cm^{-2} · s^{-1} when the cuvet was within 0.5 cm of the exit filter of the lamp. The cuvet side walls were blackened to prevent UV light from entering except though the front face, and the contents were continually stirred with a magnetic follower. The same cuvet in the same position with respect to the UV lamp was also used for the test sample, which was sufficiently dilute to present an optical density of <0.2 to the incoming irradiation. In the limit of low total optical density, molecules do not shield each other from the constant irradiation and therefore have a constant probability per unit time of undergoing conversion. Therefore photolysis becomes a first-order process with an exponential progress curve toward completion, assuming that the photolysis product does not itself undergo further photochemistry. It is readily derivable (Livingston,

1971) that the time to reach 90% conversion, $t_{90\%}$, equals $(IQ\epsilon)^{-1}$, where I is the irradiation intensity in einsteins cm^{-2} s^{-1}, Q is the quantum efficiency in mol/einstein, and ϵ is the extinction coefficient in cm^2 · (mol substrate)$^{-1}$, numerically 10^3 times the decadic extinction coefficient in conventional units of $M^{-1}cm^{-1}$. Before and at intervals during the irradiation, the UV absorbance spectrum was measured to determine the percentage conversion towards the final spectrum and thus obtain $t_{90\%}$.

Another procedure more directly tested the quantum efficiency of Ca^{2+} release from nitr-2. A solution with 1 mM nitr-2 was photolyzed with free Ca^{2+} strongly buffered at 1 μM with 10 mM diethylenetriaminepentaacetic acid (DTPA) in a pH stat at pH 7.27. The 1 μM level of free Ca^{2+} was chosen so that nearly all the unphotolyzed chelator molecules but hardly any of the photolyzed would bear Ca^{2+}. Each Ca^{2+} released would bind to H_2DTPA to form CaDTPA and release 2 H^+ to be detected continuously by the pH-stat. The UV light was introduced through the translucent floor of the titration vessel; the optical density of the 1 mM nitr-2 solution was sufficient to absorb >99% of the incident UV, whose intensity was separately calibrated with ferrioxalate in the same vessel. From the initial slope of the reaction progress curve, the initial rate of Ca^{2+} release and hence the quantum efficiency could be calculated.

Light Sources

The xenon flashlamp used both for chemical kinetics and biological experiments was a Model 5100 SP7 from Photochemical Research Associates, London, Ontario, Canada. We modified it to increase the capacitor bank to 200 μF and the charging voltage to 1.35–1.4 kV, corresponding to 182–196 joules stored. The pulse rise and fall times measured between 10% and 90% intensity levels were 0.36 and 3.7 ms respectively. The output from the lamp was an image, ~1 × 3 mm, of the xenon arc. Its effective intensity at maximum charging voltage was assessed with test droplets of about 10 mM nitr-2 plus excess EGTA or $CaCl_2$, confined under mineral oil to prevent evaporation. The droplets were approximately 100-μm diameter hemispheres, small enough to keep the absorbance near 0.3. The 380 nm transmittance of these droplets was monitored before and after successive full power flashes until no further decrease in transmittance was observable. When the flashes were filtered only by a thin sheet of glass to block shortwave UV (<300 nm), the absorbance change after the first flash corresponded to photolysis of 22% of the nitr-2 in EGTA medium or 42% of the chelator in excess Ca^{2+}. These results indicate that the wideband output of the flashlamp would be equivalent to 0.3 ± 0.08 J cm^{-2} of 350 nm irradiation in its effect on nitr-2 in a single flash.

Current transients through the flashlamp were limited by an inductor that generated a loud mechanical jolt on discharge. This inductor had to be mechanically isolated from the vibration isolation platform on which the electrophysiological apparatus was mounted. The high voltage leads (carrying 25 kV) to the flashlamp had to be carefully routed and shielded to minimize electrical interference, especially with the voltage clamp, nerve stimulating, pulse-generating, and timing circuits.

Some biological experiments used a Zeiss 75 W continuous xenon arc lamp equipped with a shutter and a quartz lens (30 mm focal length, 0.42 N.A.) to provide light pulses of several seconds duration. The focussed light intensity was equivalent to about 0.1 W/cm^2 at 350–360 nm. Care had to be taken to avoid switching on the power to this lamp during experiments, since the electromagnetic transients created were severe enough to destroy operational amplifiers in the voltage clamp and related circuitry.

Kinetics of Photolysis

Kinetics of the conversion of nitr-2 to the nitrosobenzophenone product were measured by standard methods of flash photolysis. For convenience of kinetic recording, the experiments were done in a Dialog apparatus (Garching, FRG) normally used for temperature jumps. Briefly, a steady, low intensity monitoring beam was used to record the transmittance of a nitr-2 sample at 375–385 nm before and immediately after a flash from the flashlamp coming from right angles. The time course of the increase in absorbance after the flash artifact was taken to signal the formation of the nitrosobenzophenone, which has a higher 375–385-nm absorbance than the starting chelator both in high or low [Ca^{2+}]. Because the flash is focused very differently in this kinetic apparatus compared to the electrophysiological set-up, no attempt was made to use the kinetic relaxation amplitude to calculate either the nitr-2 quantum efficiency or the flashlamp intensity.

Electrophysiological Methods

Physiological experiments were performed on single identified neurons in abdominal ganglia dissected from *Aplysia californica*. Ganglia were desheathed and pinned in a chamber containing artificial seawater as described earlier (Kramer and Zucker, 1985*a*). Tetraethylammonium (TEA) from Sigma Chemical Co. (St. Louis, MO) was checked for purity (Zucker, 1981) and added to some solutions to give a final concentration of 50 mM. Temperature was controlled at 18°C.

Nitr-2 was stored at −15°C. in a light-tight vial to prevent photolysis, though brief exposures to ordinary fluorescent room lights were not harmful. Thawed aliquots were pressure-injected into neurons using Kwik-fill capillaries (World Precision Instruments, New Haven, CT) having outside tip diameters of ~1 μm. The capillaries were backfilled with 0.5 μl of 400 mM nitr-2, 75% of which was in the calcium form with the remainder as the potassium salt. The inside of the largely empty capillary was moist enough with this conductive solution that a platinum wire inserted into the back of the electrode, but not in direct contact with the fluid at the tip, could still be used to record potentials at the tip with a microelectrode amplifier. After a cell was penetrated and a seal formed to the capillary, 2–20 nl of nitr-2 was injected with repeated pressure pulses (~300 KPa for 100 ms). For typical cells of ~300-μm diameter, this would lead to a final intracellular concentration of 8–80 mM nitr-2. However, leakage of nitr-2 into the axon probably reduced the final concentration. For ordinary visual observation of cells injected with nitr-2, the fiber optic illuminator was filtered to remove wavelengths below 450 nm to prevent photolysis of nitr-2 by ultraviolet light.

Neurons were voltage-clamped with a two-electrode clamp circuit described in Smith and Zucker (1980). Separate bath electrodes were used for voltage and current in a virtual ground circuit; this eliminated errors due to voltage drops across the bath electrode. We did not compensate for voltage drops due to the series resistance in the extracellular fluid, because membrane currents were always <1 μA, which would lead to a series resistance error of less than 1 mV in the large cells used here (Smith and Zucker, 1980; Kramer and Zucker, 1985*a*). Voltage and current levels were recorded on a Nicolet (Madison, WI) 4094 digital oscilloscope for subsequent analysis and display. Traces were plotted on a Hewlett-Packard (Palo Alto, CA) 7470A plotter.

In some experiments, we needed to measure small membrane current transients in the presence of large steady currents flowing at potentials far from the resting potential. Our protocol was to step to the membrane potential, wait several seconds until the membrane current stabilized, then actuate a circuit to sample the membrane current, hold this value, and subtract this value from subsequent signals. This produced a current signal with a baseline subtracted at the time of actuation. The traces in Figs. 9–11 begin at this time.

RESULTS

Absorbance Spectra and Ca^{2+} Affinities of Nitr-2

Before photolysis, the absorbance spectra of nitr-2 in the 330–400 nm region (Fig. 2) were practically independent of free [Ca^{2+}] and resembled that of an isolated nitropiperonyl group, with an extinction coefficient of ~4,000 $M^{-1}cm^{-1}$ at its peak at 360 nm. Below 330 nm, the spectrum responded to the addition of Ca^{2+} in a manner

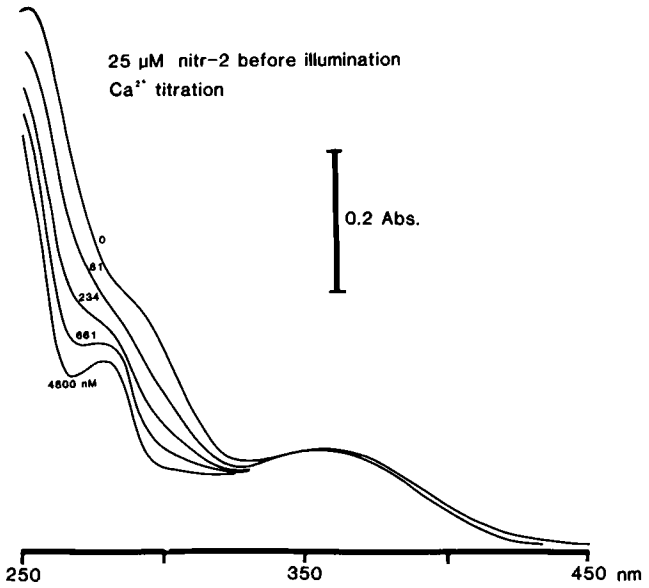

FIGURE 2 Absorbance spectra of unphotolyzed nitr-2 as a function of free [Ca^{2+}]. 25 μM nitr-2 was dissolved in 100 mM KCl, 4 mM dipotassium salt of N-(hydroxyethyl)-ethylenediamine-N,N',N'-triacetic acid (HEEDTA), 10 mM tris (hydroxymethyl)aminomethane, 2 mM MOPS, pH 8.84. The absorbance spectrum was then recorded giving the curve labeled "0." Then 2 mM $CaCl_2$ was added as well as enough concentrated KOH to raise the pH to 9.14. At this pH the calculated free [Ca^{2+}] in the buffer was 41 nM. The spectrum was recorded again. Successive additions of HCl lowered pH to 8.81 (free [Ca^{2+}] 81 nM), 8.57 (free [Ca^{2+}] 135 nM), 8.33 (free [Ca^{2+}] 234 nM), 8.10 (free [Ca^{2+}] 398 nM), 7.88 (free [Ca^{2+}] 661 nM), 7.50 (free [Ca^{2+}] 1.585 μM), and 7.03 (free [Ca^{2+}] 4.80 μM). Though absorption spectra were recorded at each pH, for clarity only every other curve has been reproduced in this figure, each being labeled by the free [Ca^{2+}] in units of nM. Addition of 3 mM extra $CaCl_2$ at the end, to raise free [Ca^{2+}] to 1 mM, produced no further spectral change, confirming that 4.79 μM free [Ca^{2+}] was already saturating. Analysis of all the absorptions at 266 nm by the usual Hill plot showed that the dissociation constant was 160 nM. All manipulations were performed under orange safelight illumination to avoid photolysis.

closely analogous to the response of the parent chelator, BAPTA, to Ca^{2+}. Thus the spectra of nitr-2 before photolysis correspond simply to the sum of the Ca^{2+}-insensitive absorbance of a nitropiperonyl group with a short-wavelength, Ca^{2+}-sensitive spectrum of BAPTA. The observed simple superposition was expected because the BAPTA and the nitropiperonyl groups are linked through a saturated carbon atom, which should act as an electronic insulator.

Analysis of the UV spectra (Fig. 2) at intermediate buffered Ca^{2+} levels showed the Ca^{2+} dissociation constant of unphotolyzed nitr-2 to be 160 nM in 0.1M KCl at 22 ± 2°C. This number is quite close to the dissociation constant for the unsubstituted parent chelator BAPTA for Ca^{2+} under the same ionic conditions, presumably because the nitropiperonyl group is only slightly electron-withdrawing. As usual for tetracarboxylate chelators, increased ionic strength markedly weakened the binding of Ca^{2+}. Thus the dissociation constant of Ca^{2+}-nitr-2 was 630 nM in 0.28M K^+, 0.1M Cl^-, HEPES added to give pH 7.30 (about 0.25

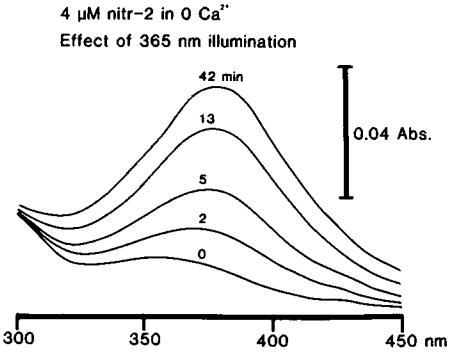

FIGURE 3 Absorbance spectra of nitr-2 undergoing photolysis in the absence of Ca^{2+}. 4 μM nitr-2 were dissolved in 130 mM KCl, 1 mM EGTA, 10 mM MOPS, brought to pH 7.2 with KOH. The curve labeled "0" was measured before any exposure of the sample to significant levels of ultraviolet radiation. (Control experiments showed that the Cary 210 spectrophotometer used negligible intensity of UV to measure these spectra.) The curves labeled "2," "5," "13," and "42 min" show the successive spectra remeasured after those durations of cumulative exposure to 365-nm irradiation at 7.8×10^{-9} einsteins · cm^{-2} · s^{-1} from the UVGL-58 lamp. Spectra were also measured at times of 1, 3, 8, 20, and 30 min but are omitted here for graphical clarity; they do confirm that the "42 min" curve represents >99% completion of the photochemical change. Solutions were at room temperature and continually stirred by a magnetic follower during illumination.

M required) at 18°C, an ionic background intended to simulate marine invertebrate axoplasm.

Upon photolysis by long-wave UV in the presence of either excess EGTA (Fig. 3) or Ca^{2+} (Fig. 4), the nitr-2 spectra changed drastically. In EGTA, photolysis

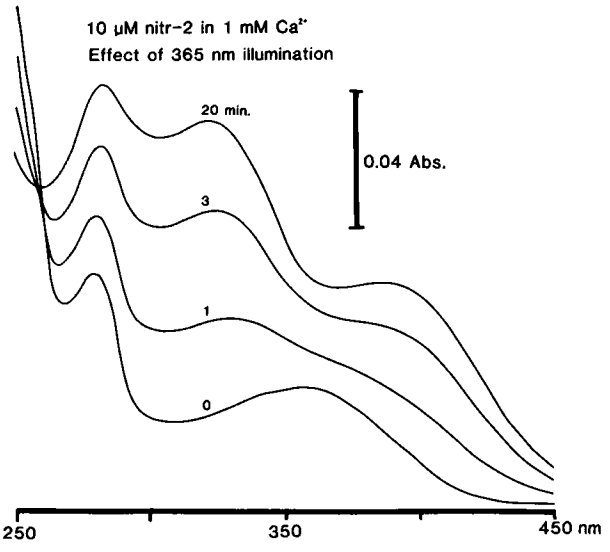

FIGURE 4 Absorbance spectra during photolysis of the Ca^{2+} complex of nitr-2. 10 μM nitr-2 were dissolved in 130 mM KCl, 1 mM $CaCl_2$, 10 mM MOPS, pH titrated to 7.2 with KOH. Spectra were obtained after 0 s, 20 s, 1 min, 2, 3, 5, 8, 13, and 20 min of 365-nm illumination, exactly as in Fig. 3. For clarity only the 0, 1, 3, and 20 min spectra have been reproduced here. The 13 min and 20 min spectra were identical, confirming completion of photolysis after those times. Photoisomerization approaches completion more rapidly here in high [Ca^{2+}] than in zero [Ca^{2+}] (Fig. 3).

increased the extinction coefficient of the 370 nm peak more than fourfold. This increase is as expected for the generation of a benzophenone whose carbonyl group is in direct conjugation with the bis(carboxymethyl)amino group para to it. This large, long-wavelength UV absorbance should be diminished when Ca^{2+} binds, since that would interfere with the ability of the amino group to donate electron density and conjugate with the carbonyl. Indeed, when free [Ca^{2+}] was raised, the 370 nm absorbance was profoundly depressed, unlike that of nitr-2 before photolysis. Titration with intermediate values of buffered [Ca^{2+}] (Fig. 5) revealed dissociation constants after photolysis of 7 μM in 0.1M KCl and 18 μM in the medium simulating marine invertebrate axoplasm. These dissociation constants are 30- to 40-fold larger than the values for the nonirradiated compound. This substantial weakening of binding upon photolysis was expected from the much greater electron-withdrawing character of a carbonyl group compared to a saturated carbon linkage, and forms the basis for the usefulness of nitr-2 for "caging" Ca^{2+}.

Photolysis Quantum Efficiency and Kinetics

The quantum efficiency of photolysis was measured with steady, nearly monochromatic UV irradiation of fairly low intensity from a simple hand mercury lamp. The progress of the photolysis was monitored by taking an absorbance spectrum every few minutes. At such low light levels, the rate of photolysis is limited by the rate of photon capture and the quantum efficiency rather than any rates of dark reactions following the initial photochemical step. Since the rate of photon capture was calculable from the optical density and the lamp intensity, the quantum efficiency was readily determined. Values of 0.03 and 0.10 were obtained in very low (excess EGTA) and high (1 mM) [Ca^{2+}] respectively.

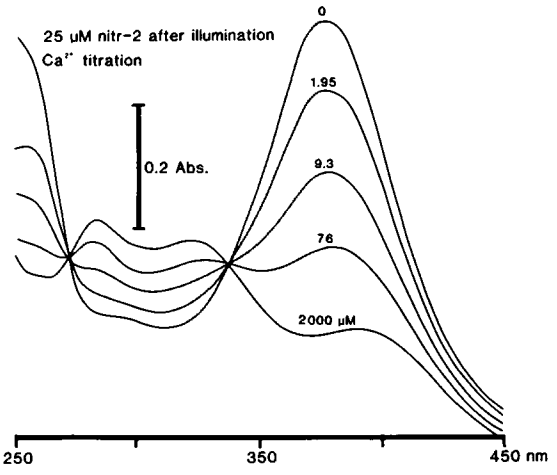

FIGURE 5 Absorbance spectra of photolyzed nitr-2 (the nitrosobenzophenone) as a function of free [Ca^{2+}]. The nitrosobenzophenone was produced by dissolving 25 μM nitr-2 in 100 mM KCl, 2 mM $CaCl_2$, 10 mM tris(hydroxymethyl)aminomethane, 2 mM MOPS, pH 8.8, and irradiating for 20 min with the UVGL-58 lamp at 365 nm to complete the photolysis. The spectrum labeled 2,000 μM was then recorded. 4 mM dipotassium salt of HEEDTA was then added, plus enough KOH to raise the pH to 10.3 (free [Ca^{2+}] < 10^{-8} M), whereupon the spectrum labeled "0" was recorded. Then HCl was added in analogy to Fig. 2, to reach the following pH and free [Ca^{2+}] values (in parentheses): 8.53 (0.117 μM), 8.13 (0.372 μM), 7.82 (0.759 μM), 7.41 (1.95 μM), 7.05 (4.57 μM), 6.77 (9.33 μM), 6.35 (26.3 μM), and 5.93 (75.8 μM). For clarity only three of these latter spectra are included in the figure. The usual Hill plot showed a dissociation constant 7 μM.

An independent value of 0.03 was obtained for the quantum efficiency of Ca^{2+} release onto DPTA at 1 μM free Ca^{2+}. This number is somewhat low compared with what would be expected from the other data above, since some 85% of the nitr-2 should have been Ca^{2+}-bound, subject to photolysis with a quantum efficiency of 0.10 and ready to lose six-sevenths of its Ca^{2+} upon conversion. The reason for the discrepancy is not known at present.

Photolyses (Fig. 3 and 4) showed very clean isosbestic points, suggesting that the reaction product was itself quite photostable. When nitr-2 was fully photolyzed in EGTA and then treated with excess Ca^{2+}, the resulting spectrum was essentially identical to that obtained by photolysis in the presence of Ca^{2+}. Likewise, photolysis in Ca^{2+} followed by chelation of Ca^{2+} by EGTA at high pH gave the same product as photolysis in EGTA throughout. Therefore Ca^{2+} influences the quantum efficiency but not the nature of the covalent bond rearrangements upon photolysis.

Fig. 6 shows a chart linking the four relevant stable states of nitr-2 (free and Ca^{2+}-bound, before and after photolysis). Unlike Fig. 1, this scheme omits the unstable photochemical intermediates between nitr-2 and the nitrosobenzophenone but recognizes the finite Ca^{2+} affinities of both.

Kinetics of Photolysis

Fig. 7 shows a record of the time course of the transmittance of a nitr-2 sample after a single flash. The decrease in

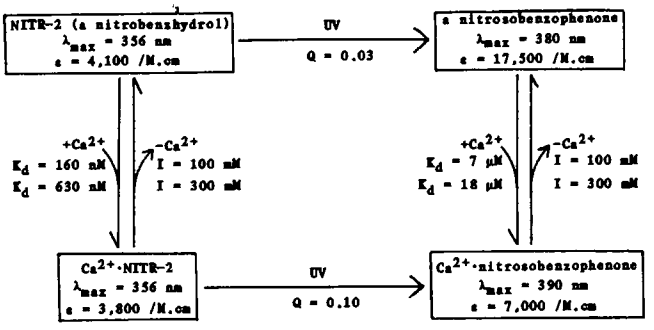

FIGURE 6 Stable states of nitr-2, their reactions with Ca^{2+}, and the photolytic effects of UV irradiation. The absorbance maximum for each species is indicated as a decadic molar extinction coefficient (ϵ) at a wavelength showing a local maximum (λ_{max}). Ca^{2+} dissociation constants (K_d) at different ionic strengths (I) and quantum efficiencies at 360 nm (Q) are indicated. These values were measured in the experiments illustrated in Figs. 2–5 (100 mM ionic strength) and in similar experiments at 300 mM ionic strength (data not illustrated).

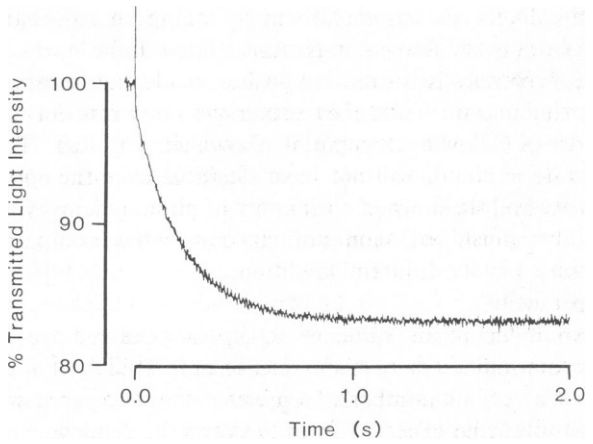

FIGURE 7 Relaxation kinetics of nitr-2 upon flash photolysis. Nitr-2 was dissolved at 50 μM in 150 mM KCL, 20 mM imidazole, 2.4 mM Ca-HEEDTA, 7.6 mM HEEDTA, pH 7.20, calculated free $[Ca^{2+}]$ = 1.0 μM. Light transmission was monitored using a tungsten source, 380 nm interference filter (10-nm bandwidth, from Ditric Optics, Marlboro, MA), silicon photodiode detector, and Biomation transient recorder. At time zero, 200 joules were discharged in a few milliseconds through the Photochemical Research Associates flashlamp, whose unfiltered output was delivered to the test solution at right angles to the monitoring beam. The resulting optical artefact is the upward spike at zero time.

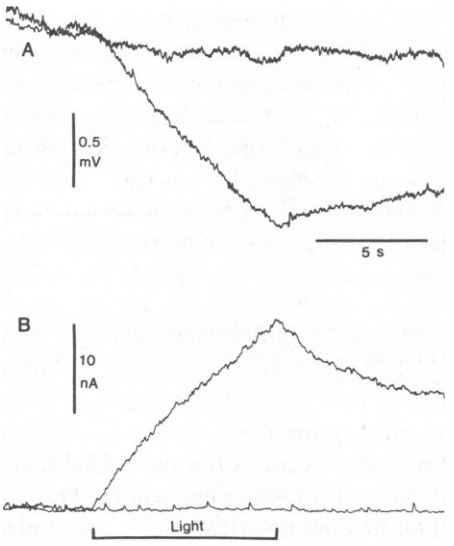

FIGURE 8 Electrophysiological responses in cell L2 (Frazier et al., 1967) injected with nitr-2 and exposed to bright light for the period indicated. (*A*) Membrane potential changes when the cell was hyperpolarized by current injection to −53 mV. (*B*) Membrane current changes when the cell was voltage clamped to −45 mV. Responses of the cell to this light before injection of nitr-2 are also shown (flat traces).

transmitted intensity after the end of the flash artifact is roughly exponential with a time constant of ~210 ms. Time constants in the range 200–250 ms at 22°C were found whether $[Ca^{2+}]$ was <10 nM (excess EGTA), 1 μM (buffered with 10 mM HEEDTA), or 2 mM, though the relaxation amplitude varies considerably, as expected. The same relaxation time constant was observed when Ca^{2+} release was monitored not by the intrinsic sensitivity of nitr-2, but by a separate indicator, azo-1 (Tsien, 1983), whose in vitro response times are known to be much faster, less than a millisecond.

Biological Tests

To demonstrate the usefulness of photo-isomerizable chelators in controlling intracellular Ca^{2+}, we injected central neurons of *Aplysia* with nitr-2 and illuminated the cells with long pulses of moderately bright light or brief flashes of intense light. We used only neurons with no photosensitivity to UV light (Arvanitaki and Chalazonitis, 1961). We monitored membrane current in these cells under voltage-clamp, and looked at the changes in membrane current caused by rises in intracellular Ca^{2+} elicited by light stimuli. Clear effects were observed in 16 cells.

Fig. 8 illustrates responses in a neuron to 8-s exposures to light from the Zeiss xenon lamp. Before injecting nitr-2, light elicited no response in the cell. After injection with nitr-2, the cell hyperpolarized continuously during the light exposure, with a peak response of ~1.2 mV. After termination of the light, the cell potential gradually returned to near its resting level, with a half time of ~15 s. Under voltage clamp, the outward current which hyperpolarized the unclamped cell was revealed. It reached a peak of 21 nA in 8 s at the holding potential of −40 mV, and declined at a rate similar to the hyperpolarization in the unclamped cell. Again, before injection of nitr-2, light had no effect on membrane current.

Responses like these were observed in almost all cells studied. They represent primarily an increase in Ca^{2+}-activated potassium current (see below).

In Fig. 9, responses to moderate light pulses and intense flashes in the same voltage-clamped cell are compared (note the difference in current scales). The response to

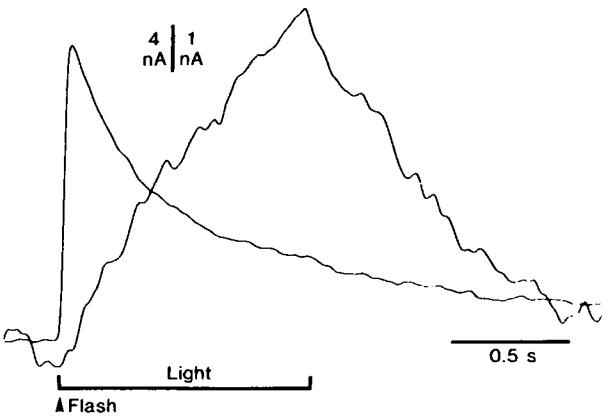

FIGURE 9 Outward currents evoked in cell L2 injected with nitr-2 (different preparation from that of Fig. 8) by 1 s of moderately bright light (slowly rising trace and right current calibration) and by an intense flash (rapidly rising trace and left current calibration). The membrane potential was clamped at 0 mV for several seconds before the light stimuli. Records start from the holding current level before the stimulus.

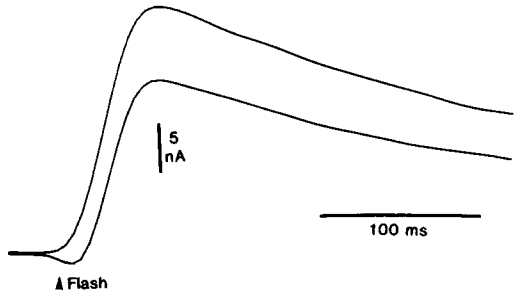

FIGURE 10 Outward currents evoked in the same cell as in Fig. 9, to the first and last of seven successive flashes, presented about once per 2 min. Membrane potential 0 mV.

prolonged light rises steadily during the light, and decays with a half-time of ~0.4 s. The flash response reaches a peak in 40 ms and decays with a half-time of about 0.3 s, slightly faster than the prolonged light response. The large difference in recovery rates in the cells illustrated in Figs. 8 and 9 gives an indication of the wide variability among cells in the rate of decay of Ca^{2+}-dependent currents following an intracellular Ca^{2+} increase.

Since light flashes not only release Ca^{2+} from nitr-2 but also exhaust the available supply of the Ca^{2+}-ligated nitrobenzhydrol, it was important to determine how constant responses to successive flashes would be. In several experiments, we found that successive responses declined by 1.6–4.6%. An example is shown in Fig. 10. Thus successive stimuli will not have identical effects, and the progressive run-down of the supply of photodynamic Ca^{2+} chelator must be taken into account when comparing responses under different conditions.

Intracellular Ca^{2+} is known to act on at least three different membrane channels in *Aplysia* central neurons (Kramer and Zucker, 1985*a*, *b*). Thus it is likely that the responses to light in normal sea water consist of a number of simultaneous effects. Fig. 11 *A* shows the dependence of membrane current responses on membrane potential in normal medium in a voltage-clamped neuron. The responses show a reversal at about −40 mV in this cell, and the reversal potential ranged from −40 mV to −60 mV in different cells, similar to the values for reversal potentials of Ca^{2+}-activated currents in these cells when Ca^{2+} is injected iontophoretically (Kramer and Zucker, 1985*b*). This is significantly higher than the potassium equilibrium potential in these cells (−75 mV, Brown and Kunze,

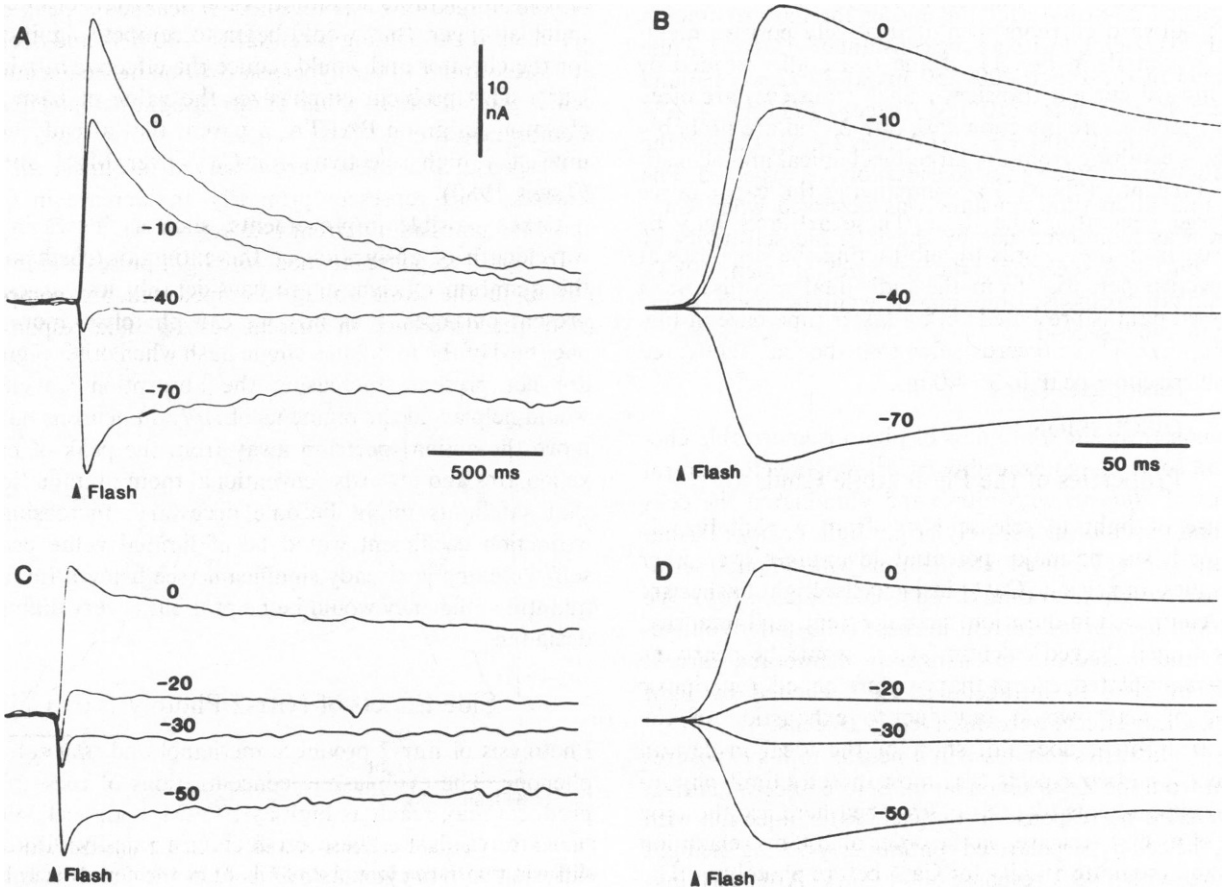

FIGURE 11 Membrane currents evoked in cell L2 injected with nitr-2 by intense light flashes. The cell was clamped to the potential shown (in mV) next to each trace. *A* and *B* show responses in normal seawater. *C* and *D* show responses in 60 mM TEA. In *B* and *D*, the response at the reversal potential is subtracted from the traces shown in *A* and *C* to remove the stimulus artifacts.

1974), and suggests that the responses are not simply due to the well-known Ca^{2+}-activated potassium current acting alone (Meech, 1978).

TEA at 50 mM can be used to block nearly all the Ca^{2+}-activated potassium channels (Hermann and Gorman, 1979). Fig. 11 *C* shows responses in the same cell after addition of TEA to the sea water. Responses now reversed at about −25 mV, similar to responses to Ca^{2+} injections in TEA (Kramer and Zucker, 1985*a*). These responses were characterized previously as due to Ca^{2+}-activated nonspecific cation channels (Kramer and Zucker, 1985*a*).

A third effect of internal Ca^{2+} is to cause inactivation of Ca^{2+} current (Eckert and Tillotson, 1981; Kramer and Zucker, 1985*b*). We do not see evidence of this effect in our responses (see Discussion).

The responses in normal seawater, which are dominated by Ca^{2+}-activated potassium current, decay about three times faster than those seen in TEA (Fig. 11, *A* and *C*). This result might reflect differences in the degree of Ca^{2+} cooperativity needed to activate Ca^{2+}-activated potassium channels and Ca^{2+}-activated nonspecific cation channels. The former may be opened by one Ca^{2+} ion, while the latter appear to require three (Barrett et al., 1982; Wong et al., 1982; Kramer and Zucker, 1985*b*).

The outward currents seen at relatively positive membrane potentials in Fig. 11, *A* and *C* are all preceded by brief inward current transients. Such transients are often seen in cells before injection with nitr-2, and are probably artefacts resulting from the large mechanical and acoustical disturbance ("bang") accompanying the capacitative discharge generating the flash. These artifacts may be removed from the records by subtracting the responses at the reversal potential from the individual records. Such processed data is presented with a faster time base in Fig. 11, *B* and *D*. These records show that the Ca^{2+} activated currents rise to a peak in 35–40 ms.

DISCUSSION

Properties of the Photolabile Chelator

The use of light to release Ca^{2+} from a photolyzable chelator has some major potential advantages over other techniques for raising $[Ca^{2+}]$ inside cells. Light flashes are easily controlled in duration, spatial extent, and intensity; with an ideal "caged calcium," Ca^{2+} would be nearly as easily manipulated, except that very prolonged elevation or release of Ca^{2+} would fail due to exhaustion of the substrate. Nitr-2 does fall short of the ideal in certain respects. The two aspects that most directly limit physiological experiments like those described here are the slow speed of its Ca^{2+} release, on the order of 200 ms relaxation time, and the finite affinity for Ca^{2+} before photolysis. The rate-limiting step after photolysis is almost certainly the loss of methanol from the hemiketal to form the nitrosobenzophenone, rather than the subsequent extrusion of Ca^{2+} itself. We know this because rate constants for Ca^{2+} dissociation from closely related chelators of similar affinity exceed $10^3\ s^{-1}$ (Kao, J., and R. Y. Tsien, manuscript in preparation); also, the slow relaxation process is still observed when nitr-2 is photolyzed in zero or saturating $[Ca^{2+}]$, conditions under which no Ca^{2+} release can be occurring. Increasing the rate of this relaxation will require judicious redesign of the molecule.

Ideally the Ca^{2+} affinity of the photolabile chelator should be so high that the chelator is practically saturated with Ca^{2+} even at resting values of cytosolic $[Ca^{2+}]$. Nearly one Ca^{2+} would then be released per chelator photolyzed. Also, molecules not yet photolyzed would minimally buffer the $[Ca^{2+}]$ rise generated by those that did photolyze. Nitr-2 falls short of this ideal, especially at high ionic strength as in marine invertebrates. Nitr-2 buffers that are significantly loaded (50–75%) with Ca^{2+} already have a high enough free $[Ca^{2+}]$ to start activating the cell (see below). A further disadvantage of insufficient Ca^{2+} affinity arises because free nitr-2 molecules happen to photolyze with some threefold lower quantum efficiency than Ca^{2+}-bound. Unfortunately, raising the Ca^{2+} affinity significantly is a major challenge for the molecular designer, especially because little increase in Mg^{2+} or H^+ affinity is tolerable. If affinities for the latter ions became much stronger, they would begin to compete significantly for the chelator and would reduce the effective affinity for Ca^{2+}. This problem emphasizes the value of basing the chelator design on BAPTA, a parent that already has an unusually high selectivity for Ca^{2+} over Mg^{2+} and H^+ (Tsien, 1980).

Other possible improvements, such as increasing the wavelength of absorption or the extinction coefficient or the quantum efficiency, are considerably less urgent for present purposes. Presently we can photolyze more than one third of the nitr-2 in a single flash when other pigments are not present. Increasing the absorption wavelength would help avoid the pigments of *Aplysia* neurons but also move the action spectrum away from the peak of pulsed xenon arcs and towards conventional room illumination, so that safelights might become necessary. Increasing the extinction coefficient would be of limited value because self-screening is already significant (see below). Increased quantum efficiency would be helpful but is very difficult to design in.

Side Effects of Nitr-2 Photolysis on Cells

Photolysis of nitr-2 produces methanol and nitrosobenzophenone. The cytoplasmic concentrations of these photoproducts may reach as high as 10 mM at the cell surface just after a flash. These products are rapidly diluted by diffusion both in cytoplasm and out of the cell. It is unlikely that the transient exposure to this concentration of methanol has any significant effect on the resting cell membrane or excitable membrane proteins (Armstrong and Binstock,

1964; Moore et al., 1964). In preliminary experiments, we found no effect of 10 mM methanol added to the external medium on inward or outward currents under voltage clamp.

The nitrosobenzophenone formed is also unlikely to be pharmacologically responsible for the effects seen, since the diaryl substitution on the ketone renders that carbonyl group far less reactive than those in *o*-nitrosoacetophenone or *o*-nitrosobenzaldehyde. These are the byproducts of photolyzing caged ATP (Kaplan et al., 1978) and cyclic nucleotides (Nargeot et al., 1983) respectively, and have been found to be relatively innocuous.

Quantifying the Effect of a Light Flash

Calculating the effect of a light flash on the intracellular free $[Ca^{2+}]$ is both important and difficult. The calculation requires quantitative knowledge of several factors, which are presently only very roughly known: (*a*) the concentration of nitr-2 in injected cells, (*b*) the proportion of nitr-2 that is bound to Ca^{2+} (some of the Ca^{2+} bound to the injected nitr-2 may be pulled off by the cell's native buffers), (*c*) the intensity of light reaching the cytoplasm, (*d*) the degree of uniformity of the light intensity in different parts of the cell, and (*e*) the magnitude and nature of native Ca^{2+} buffering.

An estimate of the effect of the light reaching the cytoplasm on intracellular Ca^{2+} may be obtained from the fact that light flashes convert ~3% of the injected Ca^{2+}-nitrobenzhydrol complex to nitrosobenzophenone. We assume that *Aplysia* neurons contain a native cytoplasmic Ca^{2+} buffer with a 25 μM dissociation constant (Alemà et al., 1973); 1.25 mM of this buffer would produce a bound-to-free $[Ca^{2+}]$ ratio of 50 (Smith and Zucker, 1980). Suppose that a cell contains 30 mM of nitrobenzhydrol, 22.5 mM bound to Ca^{2+} and 7.5 mM free. Assuming a dissociation constant of 630 nM, and using the equations of Zucker and Steinhardt (1978) for competing buffer systems, we calculate the free $[Ca^{2+}]$ to be 1.89 μM. If a light flash converts 3% of the bound nitrobenzhydrol to nitrosobenzophenone, 0.675 mM of the latter will be produced and the former will drop to 21.825 mM. Considering the relative quantum efficiencies of the bound and free nitrobenzhydrols, 1% of the free nitrobenzhydrol, or 0.075 mM, will be photolyzed to nitrosobenzophenone, leaving 7.425 mM free nitrobenzhydrol. Knowing the concentrations of total nitrobenzhydrol (29.95 mM), nitrosobenzophenone (0.75 mM), native buffer (1.25 mM), and total Ca^{2+} (22.5 mM), and the dissociation constants for the two forms of nitr-2 and the native buffer, the free $[Ca^{2+}]$ may be calculated as 2.03 μM. Because the high concentration of nitr-2 overwhelms the cell's native buffer, errors in estimating the capacity or affinity of this buffer have little effect on the calculations. Thus, we estimate that a single light flash causes a transient elevation of intracellular free $[Ca^{2+}]$ of ~140 nM (Fig. 12).

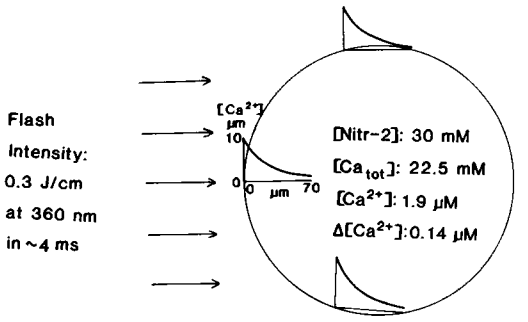

FIGURE 12 Diagram showing estimated injected nitr-2 and total Ca^{2+} concentrations, calculated free $[Ca^{2+}]$ and flash-evoked $[Ca^{2+}]$ increment, and the spatial decay of the $[Ca^{2+}]$ increment just after the flash at the cell surface facing the light source.

Since our flashlamp photolyzed about 40% of bound nitrobenzhydrol per flash in small droplets of dilute nitr-2, it might seen surprising that only ~3% was photolyzed in cells exposed to the same flash. However, this result is expected when we consider that 30 mM Ca-nitr-2 absorbs UV light at 360 nm with a decadic absorbance coefficient of 120/cm. To this must be added an absorbance coefficient of *Aplysia* cytoplasm, which we have measured at ~25/cm at 360 nm. We calculate that a 300-μm diameter neuron will experience a volume-average intensity only one-seventh as great as the incident light intensity. Combined with extra absorption of light by Schwann cells surrounding the neuron, and loss of light due to surface scattering, we expect nitr-2 photolysis in neurons at about one-tenth the rate obtainable in low-absorbance droplets. As the nitr-2 concentration in a cell is increased, the fraction of nitr-2 photolyzed by a flash decreases.

The spatial decay of light intensity in a neuron injected with nitr-2 has important implications for the distribution of Ca^{2+} released in a neuron after a flash. At the surface facing the flash lamp, the incident light intensity should be similar to that achieved in low-absorbance droplets, and up to 40% of the Ca-nitr-2 and 15% of the free nitr-2 would be photolyzed by a flash. There the nitr-2 concentration should transiently drop to 20 mM, and the nitrosobenzophenone concentration transiently rise to 10 mM right after the flash, producing a local free $[Ca^{2+}]$ of ~10 μM under the surface which decays spatially to 5 μM in ~30 μm and to 2.7 μM in ~70 μm. This peak level of submembrane Ca^{2+} is similar to levels attained during Ca^{2+} influx through voltage-dependent Ca^{2+} channels (Smith and Zucker, 1980). Thus the Ca^{2+} released is *not* uniformly distributed inside the neuron, but is concentrated in the general vicinity of the surface facing the light source. The initial $[Ca^{2+}]$ transient will be uniformly high near this hemispheric surface right after the flash, and will be negligible at most of the opposite surface. Ca^{2+} will subsequently equilibrate by diffusion to the opposite pole of the cell, and unphotolyzed nitr-2 will diffuse toward the front of the cell and chelate some of the released Ca^{2+}.

Thus, although the average Ca^{2+} transient is only 7% the magnitude of the resting Ca^{2+} in an injected cell, the Ca^{2+} under half the membrane surface increases transiently to about five times the resting level (see Fig. 12).

These considerations are important for understanding the time course of cell processes modulated by Ca^{2+}. In particular, the decay of Ca^{2+}-dependent membrane current will not simply reflect the removal of Ca^{2+} from cytoplasm. Rather, it will also be influenced by Ca^{2+} diffusion away from the hemisphere facing the light (and toward the opposite membrane), and by the redistribution of nitr-2 in the cell. These processes will speed the decay of flash-evoked responses compared to responses to prolonged light exposures (see Fig. 9). For example, suppose nitr-2 has a diffusion coefficient of 10^{-7} cm^2 s^{-1} and is activated by a flash only at the very surface. This nitr-2 will diffuse inwardly ~1 μm within 40 ms, well before most of the calcium has been released. At the surface, the concentration of the photolysed nitr-2 would drop at 40 ms to one-sixth its value 1 ms after the flash. We think that these aspects of Ca^{2+} and nitr-2 diffusion help to account for the unexpectedly rapid (40 ms) time to peak in Ca^{2+}-activated membrane currents (Fig. 11), despite the relatively slow (~200 ms) time constant of the photo-isomerization of nitr-2.

The computations in Fig. 12 apply only to the first flash seen by a cell. Subsequent flashes will have quantitatively different effects, because the starting concentrations of free calcium and free and calcium-bound nitrobenzhydrol and nitrosobenzophenone will all be different, the highly absorbent nitrosobenzophenone will screen more of the incident light from cytoplasmic nitrobenzhydrol, and the cell will have had time to pump out more of the calcium which had been injected. It will be necessary to take all these changes into account when attempting to predict responses to repeated light flashes.

The Resting Level of Free Calcium

We wished to control effectively and quantitatively the intracellular Ca^{2+} in cells, to prevent the removal of injected Ca^{2+} by native extrusion and uptake pumps, and to maximize the amount of Ca^{2+} released in response to light. To accomplish these goals, cells must be injected with a high concentration of nitr-2 that is heavily loaded with Ca^{2+} (i.e., where most of the nitr-2 is in the Ca^{2+} form). We calculate that we inject about 30 mM of nitr-2 with 75% bound to Ca^{2+} and 25% in the uncomplexed form, which has a free Ca^{2+} level of 1.9 μM. This is substantially higher than measured values of free [Ca^{2+}] in resting *Aplysia* neurons (180 nM, Gorman et al., 1984), and it might be expected that our neurons are not behaving exactly as uninjected neurons would act.

There are two indications that this is the case: (*a*) In some neurons, injection of nitr-2 was accompanied by a gradual hyperpolarization of the cell by a few mV. This is unlikely to be due to membrane damage, which would lead to a depolarization. Rather, it probably reflects a tonic activation of some Ca^{2+}-activated potassium current. (*b*) Cells filled with nitr-2 displayed little inactivation of inward Ca^{2+} current in response to depolarizing pulses in TEA. This effect is similar to the block by EGTA injection of Ca^{2+} inactivation (Eckert and Tillotson, 1981), and indicates that Ca^{2+} entering through membrane channels is buffered effectively by nitr-2.

It is remarkable that we saw no sign of a Ca^{2+}-dependent block of Ca^{2+} current (Eckert and Tillotson, 1981; Kramer and Zucker, 1985*b*) in response to light flashes. Even when the predominant Ca^{2+}-activated potassium current was blocked with TEA, the remaining light-evoked current behaved like the Ca^{2+}-activated nonspecific cation current (Kramer and Zucker, 1985*a*). We saw no contribution from a Ca^{2+}-dependent block of pre-existing Ca^{2+} current, which would probably have appeared as a slow outward current following the inward nonspecific cation current. Either Ca^{2+} inactivation is less sensitive to intracellular Ca^{2+} than the other Ca^{2+}-activated currents, or the Ca^{2+} inactivation process is already fully saturated by micromolar calcium.

It should be noted that the problems of optical screening and inadequate pre-photolysis affinity for Ca^{2+} are particularly severe in *Aplysia* neurons with their large size, intrinsic pigments, and high ionic strength. Vertebrate cells generally have much shorter path lengths, less pigmentation, and a lower ionic strength that would give much stronger binding of nitr-2 to Ca^{2+}.

We thank Dr. Joseph Kao for assistance with the nitr-2 kinetic measurements, and Mr. Russell English for valuable electronic assistance.

This work was supported by National Institutes of Health grants NS-15114 to R. S. Zucker, and GM-31004, EY-04372, and a Searle Scholars Award to R. Y. Tsien.

Received for publication 13 February 1986 and in final form 16 June 1986.

REFERENCES

Alemà, S., P. Calissano, G. Rusca, and A. Giuditta. 1973. Identification of a calcium-binding, brain specific protein in the axoplasm of squid giant axons. *J. Neurochem.* 20:681–689.

Armstrong, C. M., and L. Binstock. 1964. The effects of several alcohols on the properties of the squid giant axon. *J. Gen. Physiol.* 48:265–277.

Arvanitaki, A., and N. Chalazonitis. 1961. Excitatory and inhibitory processes initiated by light and infra-red radiations in single identifiable nerve cells (giant ganglion cells of *Aplysia*). *In* Nervous Inhibition. E. Florey, editor. Pergamon Press, New York. 194–231.

Barrett, J. N., K. L. Magleby, and B. S. Pallotta. 1982. Properties of single calcium-activated potassium channels in cultured rat muscle. *J. Physiol. (Lond.).* 331:211–230.

Brown, A. M., and D. L. Kunze. 1974. Ionic activities in identifiable *Aplysia* neurons. *In* pH and Ion-Selective Microelectrodes. H. Berman and N. Hebert, editors. Plenum Publishing Corp., New York. 57–73.

Bygrave, F. L. 1978. Mitochondrial calcium transport. *Curr. Top. Bioenerg.* 8:259–318.

Corson, D. W., and A. Fein. 1983. Quantitative pressure injection of

picoliter volumes into *Limulus* ventral photoreceptors. *Biophys. J.* 44:299–304.

Curtis, D. R. 1964. Microelectrophoresis. *In* Physical Techniques in Biological Research. Vol. 5: Electrophysiological Methods. Part A. W. L. Nastuk, editor. Academic Press, Inc., New York. 144–190.

DiPolo, R., H. Rojas, J. Vergara, R. Lopez, and C. Caputo. 1983. Measurements of intracellular ionized calcium in squid giant axons using calcium-selective microelectrodes. *Biochem. Biophys. Acta.* 728:311–318.

Eckert, R., and D. Tillotson. 1981. Calcium-mediated inactivation of the calcium conductance in caesium-loaded giant neurones of *Aplysia californica*. *J. Physiol. (Lond.).* 314:265–280.

Frazier, W. T., E. R. Kandel, I. Kupfermann, R. Waziri, and R. E. Coggeshall. 1967. Morphological and functional properties of identified neurons in the abdominal ganglion of *Aplysia californica*. *J. Neurophysiol.* 30:1288–1351.

Gorman, A. L. F., S. Levy, E. Nasi, and D. Tillotson. 1984. Intracellular calcium measured with calcium-sensitive micro-electrodes and arsenazo III in voltage-clamped *Aplysia* neurones. *J. Physiol. (Lond.).* 353:127–142.

Grynkiewicz, G., M. Poenie, and R. Y. Tsien. 1985. A new generation of Ca^{2+} indicators with greatly improved fluorescence properties. *J. Biol. Chem.* 260:3440–3450.

Hagiwara, S., and L. Byerly. 1981. Calcium channel. *Annu. Rev. Neurosci.* 4:69–125.

Hatchard, C. G., and C. A. Parker. 1956. A new sensitive chemical actinometer. II. Potassium ferrioxalate as a standard chemical actinometer. *Proc. R. Soc. Lond. A. Phys. Sci.* 235:518–536.

Hermann, A., and A. L. F. Gorman. 1979. External and internal effects of tetraethylammonium on voltage-dependent and Ca-dependent K^+ currents components in molluscan pacemaker neurons. *Neurosci. Letts.* 12:87–92.

Kaplan, J. H., B. Forbush, III, and J. F. Hoffman. 1978. Rapid photolytic release of adenosine 5'-triphosphate from a protected analogue: utilization by the Na:K pump of human red blood cell ghosts. *Biochemistry.* 17:1929–1935.

Kramer, R. H., and R. S. Zucker. 1985*a*. Calcium-dependent inward current in *Aplysia* bursting pace-maker neurones. *J. Physiol. (Lond.).* 362:107–130.

Kramer, R. H., and R. S. Zucker. 1985*b*. Calcium-induced inactivation of calcium current causes the inter-burst hyperpolarization of *Aplysia* bursting neurones. *J. Physiol. (Lond.).* 362:131–160.

Lester, H. A., and J. M. Nerbonne. 1982. Physiological and pharmacological manipulations with light flashes. *Annu. Rev. Biophys. Bioeng.* 11:151–175.

Liu, C.-M., and T. E. Hermann. 1978. Characterization of ionomycin as a calcium ionophore. *J. Biol. Chem.* 253:5892–5894.

Livingston, R. 1971. Behavior of photochromic systems. *In* Techniques of Chemistry. Vol. 3: Photochromism. G. H. Brown, editor. John Wiley & Sons, New York. 13–44.

Martell, A. E., and R. M. Smith. 1974. Critical Stability Constants. Vol. 1. Plenum Publishing Corp., New York.

Meech, R. W. 1978. Calcium-dependent potassium activation in nervous tissues. *Annu. Rev. Biophys. Bioeng.* 7:1–18.

Moore, J. W., W. Ulbricht, and M. Takata. 1964. Effect of ethanol on the sodium and potassium conductances of the squid axon membrane. *J. Gen. Physiol.* 48:279–295.

Nargeot, J., J. M. Nerbonne, J. Engels, and H. A. Lester. 1983. Time course of the increase in the myocardial slow inward current after a photochemically generated concentration jump of intracellular cAMP. *Proc. Natl. Acad. Sci. USA.* 80:2395–2399.

Noyori, R., S. Murata, and M. Suzuki. 1981. Trimethylsilyl triflate in organic synthesis. *Tetrahedron.* 37:3899–3910.

Patchornik, A., B. Amit, and R. B. Woodward. 1970. Photosensitive protecting groups. *J. Am. Chem. Soc.* 92:6333–6335.

Pillai, V. N. R. 1980. Photoreversable protecting groups in organic solutions. *Synthesis.* 1980:1–26.

Reed, P. W., and H. A. Lardy. 1972. A23187: a divalent cation ionophore. *J. Biol. Chem.* 21:6970–6977.

Smith, S. J., and R. S. Zucker. 1980. Aequorin response facilitation and intracellular calcium accumulation in molluscan neurones. *J. Physiol. (Lond.).* 300:167–196.

Tsien, R. Y. 1980. New calcium indicators and buffers with high selectivity against magnesium and protons: design, synthesis, and properties of prototype structures. *Biochemistry.* 19:2396–2404.

Tsien, R. Y. 1983. Intracellular measurements of ionic activities. *Annu. Rev. Biophys. Bioeng.* 12:91–116.

Wong, B. S., H. Lecar, and M. Adler. 1982. Single calcium-dependent potassium channels in clonal anterior pituitary cells. *Biophys. J.* 39:313–317.

Zucker, R. S. 1981. Tetraethylammonium contains an impurity which alkalizes cytoplasm and reduce calcium buffering in neurons. *Brain Res.* 208:473–478.

Zucker, R. S., and R. A. Steinhardt. 1978. Prevention of the cortical reaction in fertilized sea urchin eggs by injection of calcium-chelating ligands. *Biochim. Biophys. Acta.* 541:459–466.